Separation of Carbon Dioxide by Asymmetric Hollow Fiber Membrane of Cellulose Triacetate

E. SADA, H. KUMAZAWA,* J.-S. WANG, and M. KOIZUMI

Department of Chemical Engineering, Kyoto University, Kyoto 606-01, Japan

SYNOPSIS

Permeation behavior of pure CO_2, O_2, and N_2 and separation characteristics of CO_2–air mixtures were examined using hollow fiber modules of asymmetric cellulose triacetate membrane at 30°C. The ideal separation factor for CO_2 relative to N_2 ranged from 21 to 24. Permeation behavior for pure CO_2 was interpreted in terms of the total immobilization model, i.e., a limiting case of the dual-mode mobility model for glassy polymer, where the diffusion coefficient for Henry's law mode is not assumed to be constant and depends on gas pressure via a modified free-volume model. Based on pure gas permeabilities to CO_2, O_2, and N_2, simulation for the separation of CO_2–air mixtures was made using a countercurrent plug flow model, and the result fitted the corresponding experimental data fairly well. Membrane plasticization induced by CO_2 had negligible effect on permeation to mixture of CO_2 and air in the range of CO_2 composition up to 50% and upstream total pressure up to 1.5 MPa.

INTRODUCTION

Nowadays the global warming issue caused by greenhouse gases has become a matter of great concern, and carbon dioxide has widely been recognized as one of the most affecting greenhouse gases. Industry is one of the major sources of CO_2. Many plants such as fossile-fuel-fired power plants, iron and steel works, and cement works discharge a huge amount of CO_2 day after day. Since CO_2 emission will increase with energy consumption, intensive efforts must be made toward energy conservation and promotion of energy efficiency. Furthermore, the processes for removal, recovery, and fixation of CO_2 emitted from stationary sources are of increasing importance.

The use of membrane technology for industrial gas separations has been shown to be practical and economical. Among many kinds of polymer membranes, cellulose triacetate membrane is known for its high permeability to CO_2. In the present work, we investigated the possibility of separating CO_2 and air mixture with asymmetric hollow fiber membrane module of cellulose triacetate. This has been done by measuring permeation rates through the hollow fibers for pure CO_2, O_2, and N_2, and carrying out separation experiments for CO_2–air mixtures. Permeabilities for the pure gases and separation factors for CO_2 relative to N_2 were calculated then. Simulation results for the mixtures based on a countercurrent plug flow model using permeation data of the pure gases were successfully compared with the experimental results. The plasticization effect of dissolved CO_2 on permeation behavior of CO_2–air mixture was also considered.

EXPERIMENTAL

Permeation and separation experiments were carried out using a membrane permeator of hollow fiber type. The details of the permeator were described elsewhere.[1] The unit consists of a bundle of asymmetric hollow fibers. An asymmetric hollow fiber of cellulose triacetate membrane has the skin layer on the outer surface, and the feed-outside operation mode was employed. That is, the feed gas is on the skin side of the asymmetric membrane.

Asymmetric hollow fiber modules of cellulose triacetate were provided by Toyobo Co. Ltd., Japan. Four modules with different dimensions have been used in the experiments. The module specification

* To whom correspondence should be addressed.

Journal of Applied Polymer Science, Vol. 45, 2181–2186 (1992)
 CCC 0021-8995/92/122181-06$04.00

Table I Dimensions of Membrane Modules

Sample No.	11	12	13	31
D_o (mm)	0.148	0.184	0.178	0.156
D_i (mm)	0.056	0.091	0.087	0.063
L_t (cm)	22	20	21	26
N_t	180	240	240	270
A_t (cm^2)	184	278	282	338

is shown in Table I. Samples 11 and 31 are similar in outer and internal diameters of hollow fibers but are different in the total outer surface (permeation) area. Samples 12 and 13 are similar in the total outer surface area as well as the outer and internal diameters. The thickness of asymmetric membrane portion in all of four modules is nearly the same, ranging from 0.0455 to 0.0465 mm.

First, permeation experiments were conducted for pure CO_2, O_2, and N_2. Then, mixtures of CO_2 and air containing 10, 20, and 50% CO_2 were permeated, and separation behavior was investigated. The composition of the permeates was determined by a gas chromatograph with a 2.5-m-long column packed with Porapak Q. The column temperature was held at 50°C, and helium was used as the carrier gas.

For the sake of comparison with permeation and separation behavior of asymmetric hollow-fiber-type membranes, experiments with the above-mentioned gases were also performed using flat homogeneous dense membranes of the same cellulose triacetate. The permeation cell is the same one as in our previous work.[2] The permeation area of the cell is 19.6 cm^2. Cellulose triacetate samples were supplied by Fuji Film Co. Ltd., Japan. The nominal thickness of the film is 50 μm (FT 0.05). The permeation rate for CO_2 was calculated by flowing helium as a pickup gas at a prescribed rate on the downstream side and determining the concentration of CO_2 by means of the gas chromatograph. The flow rate of pickup gas was adjusted so that the partial pressure of CO_2 might be regarded substantially as zero.

All of the experiments were carried out at 30°C and upstream total pressure up to 2.4 MPa for pure gases and 1.5 MPa for gas mixtures.

EXPERIMENTAL RESULTS AND DISCUSSION

Permeation to Pure Gas

Measured steady-state permeation rate for pure gases were converted to the permeation rate coefficients defined by

$$\kappa = \frac{\bar{P}}{\delta} = \frac{J_s}{p_2 - p_1} \quad (1)$$

where $\bar{P}$ refers to the mean permeability coefficient and δ to the thickness of the skin layer of the asymmetric hollow fiber membrane. The permeation rate coefficients for N_2, O_2, and CO_2 in asymmetric hollow fiber modules 11, 12, and 31 were plotted against the difference between pressures of feed and permeate sides in Figure 1. The coefficients for O_2 and N_2 are shown to be almost independent of the pressure difference, whereas those for CO_2 increase with increasing pressure difference. For the four modules, values of the permeation rate coefficients for CO_2, O_2, and N_2 in the limit of $\Delta p \to 0$, and separation factors defined as the ratio $(\bar{P}/\delta)_{\Delta p \to 0}$ for CO_2 to N_2 are listed in Table II. The separation factors for modules 11, 12, and 13 range from 21 to 24. The separation factor for sample 31 is determined to be 17. This may be because the morphology of the skin layer of sample 31 is different from those of the other modules.

In order to find out whether the above-mentioned pressure dependence is caused by membrane material (cellulose triacetate) or just by module geometry, mean permeability coefficients for these three gases through a flat homogeneous membrane

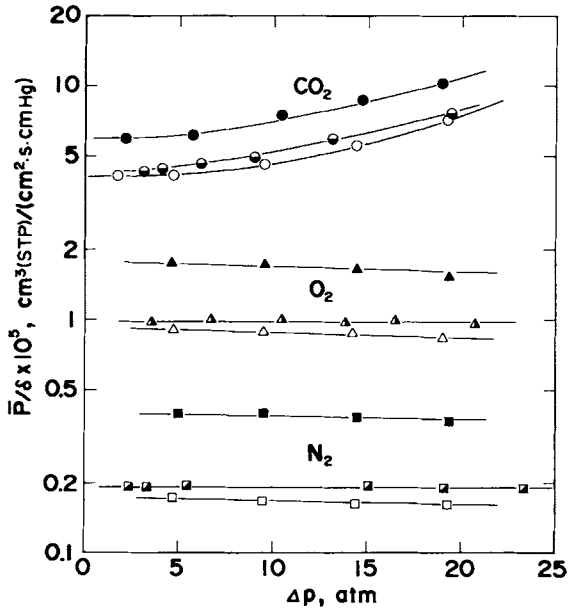

Figure 1 Permeation rate coefficients as a function of pressure difference for CO_2, O_2, and N_2 in asymmetric hollow fibers of cellulose triacetate [sample no. 11 (half filled keys), no. 12 (open keys), no. 31 (filled keys)] at 30°C.

Table II Permeation Rate Coefficients[a] for CO_2, O_2, and N_2 and Separation Factors[b] for CO_2 Relative to N_2 in Hollow Fiber Membrane Modules at 30°C

	No. 11	No. 12	No. 13	No. 31
$(\bar{P}/\delta)_{CO_2} \times 10^5$	4.5	4.0	6.2	6.1
$(\bar{P}/\delta)_{O_2} \times 10^5$	1.0	0.90	1.5	1.8
$(\bar{P}/\delta)_{N_2} \times 10^5$	0.20	0.17	0.29	0.39
α	22	24	21	17

[a] Values at the limit of $\Delta p \to 0$, [cm^3 (STP)/(cm^2 s cmHg)].
[b] $\alpha = (\bar{P}/\delta)_{CO_2}/(\bar{P}/\delta)_{N_2}$.

of cellulose triacetate were measured and plotted versus pressure difference, as shown in Figure 2. For N_2 and O_2, the mean permeability coefficients are found to be essentially constant, and in the case of CO_2 the coefficients increase with increasing pressure difference. This result conforms to the permeation results of the hollow fiber membrane module. In Table III, together with permeability coefficients for CO_2, O_2, and N_2 in the limit of $\Delta p \to 0$, the value of the ideal separation factor of the homogeneous membrane defined as the ratio of permeability for CO_2 to that for N_2 is listed.

The pressure dependence of $\bar{P}/\delta$ and $\bar{P}$ for CO_2 here seems to reflect plasticization effect induced by dissolved CO_2 and can be simulated in terms of the total immobilization model in conjunction with a modified free-volume model.[3,4] That is, the total immobilization model, one limiting case of the dual-mode mobility model is operative, where the diffusion coefficient for Henry's law mode is not assumed to be constant but depends on the gas pressure in terms of the modified free-volume model. According to such a model, the pressure dependence of the permeability coefficient should be linear or quadratic,[5] and therefore conforms to the experimental results for CO_2 depicted in Figures 1 and 2.

Table III Permeability Coefficients[a] for CO_2, O_2, and N_2 and Separation Factors[b] for CO_2 Relative to N_2 in a Flat Homogeneous Membrane at 30°C

$\bar{P}_{CO_2}$	6.4×10^{-10}
$\bar{P}_{O_2}$	6.8×10^{-11}
$\bar{P}_{N_2}$	2.0×10^{-11}
α	32

[a] Values at the limit of $\Delta p \to 0$, [cm^3 (STP) cm/(cm^2 s cmHg)].
[b] $\alpha = \bar{P}_{CO_2}/\bar{P}_{N_2}$.

Permeation for CO_2–Air Mixtures

Typical separation results for the CO_2–air mixture containing 10 vol % CO_2 are indicated in Figure 3 as a plot of concentration of CO_2 in permeate stream (y_P) versus stage cut (defined as the fraction of the feed that has permeated). Permeability measurements were carried out at three feed pressure levels with constant permeate pressure (1 atm).

As shown in this figure, permeate with higher CO_2

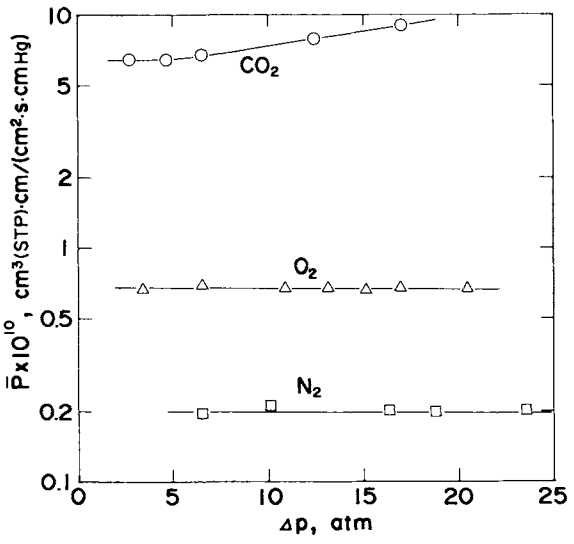

Figure 2 Permeability coefficients as a function of pressure difference for CO_2, O_2, and N_2 in a flat homogeneous membrane of cellulose triacetate at 30°C.

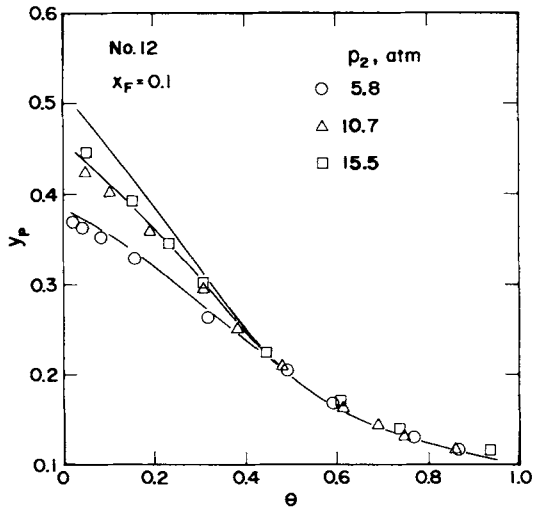

Figure 3 Relationship between mole fraction of CO_2 in the permeate stream and stage cut at different upstream total pressures for a mole fraction of CO_2 of 0.1 in upstream (sample no. 12).

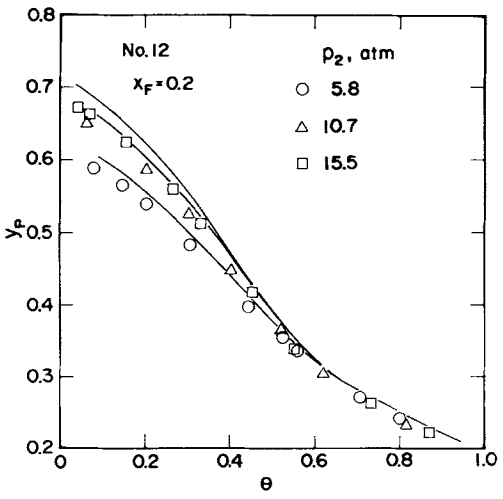

Figure 4 Relationship between mole fraction of CO_2 in the permeate stream and stage cut at different upstream total pressures for a mole fraction of CO_2 of 0.2 in upstream (sample no. 12).

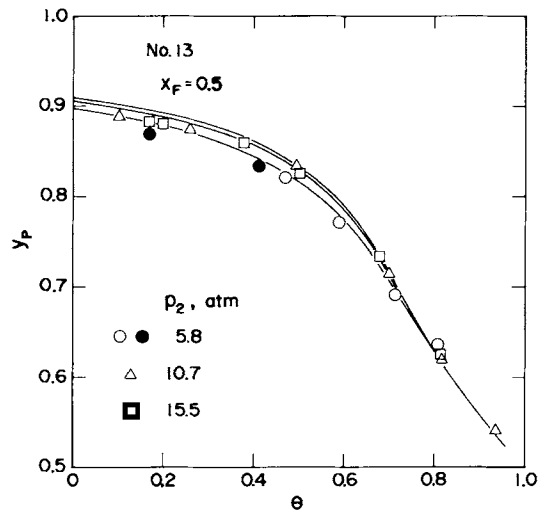

Figure 5 Relationship between mole fraction of CO_2 in the permeate stream and stage cut at different upstream total pressures for a mole fraction of CO_2 of 0.5 in upstream (sample no. 13).

concentration could be obtained at the same stage cut as the feed pressure was raised from 5.8 to 10.7 atm. Although the degree of this increase diminished as the feed pressure was raised further to 15.5 atm, higher permeation flux with unchanged separation factor was achieved. This is understandable if the permeabilities for penetrants remain the same as in their pure-gas cases, and no plasticization due to CO_2 takes place (this will be discussed later).

The solid curves are simulation results using a simple countercurrent plug flow model,[6] where the high- and low-pressure gas streams flow countercurrently to one another, and the total pressure is uniform in both the streams. A CO_2–air mixture is treated as a ternary system of CO_2, O_2, and N_2, and their pure-gas permeabilities are used in the calculation. The lower, middle and upper solid curves represent simulation results, respectively, for the feed pressures of 5.8, 10.7, and 15.5 atm.

Simulation results for CO_2–air mixtures containing 20 and 50% CO_2 are shown as solid curves in Figures 4 through 6 in comparison with experimental points. Similarly, the solid curves from the bottom upward represent simulation results for the feed pressures in order. It can be seen that, except in low stage cut region where some deviation appears, the agreement between simulation results and experimental data is satisfactory.

The separation experiments were carried out from low to high pressure through the three pressure levels. After the highest pressure, 15.5 atm, measurements were repeated at a low-pressure level to see whether some change would occur or not. The point is that if under high partial pressure of CO_2 the membrane might be plasticized, then the permeabilities for O_2 and N_2 would increase.[7] In this case it follows that the separation factor or y_P might decrease.[8,9] As indicated in Figures 5 and 6 by filled circles representing the data obtained from such repetition, even in the case of 50% CO_2 mixture where CO_2 partial pressure is up to about 8 atm, no change was detected.

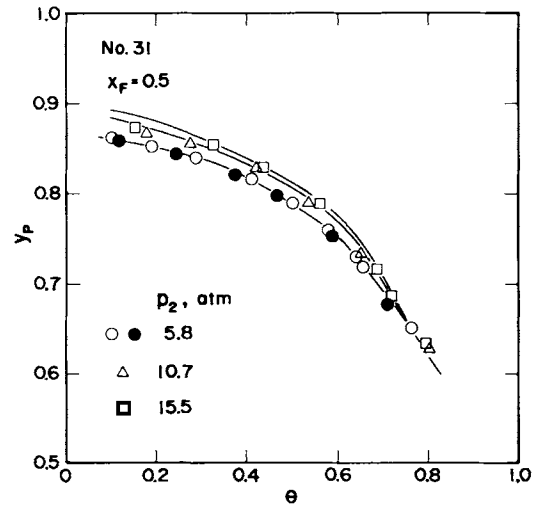

Figure 6 Relationship between mole fraction of CO_2 in the permeate stream and stage cut at different upstream total pressures for a mole fraction of CO_2 of 0.5 in upstream (sample no. 31).

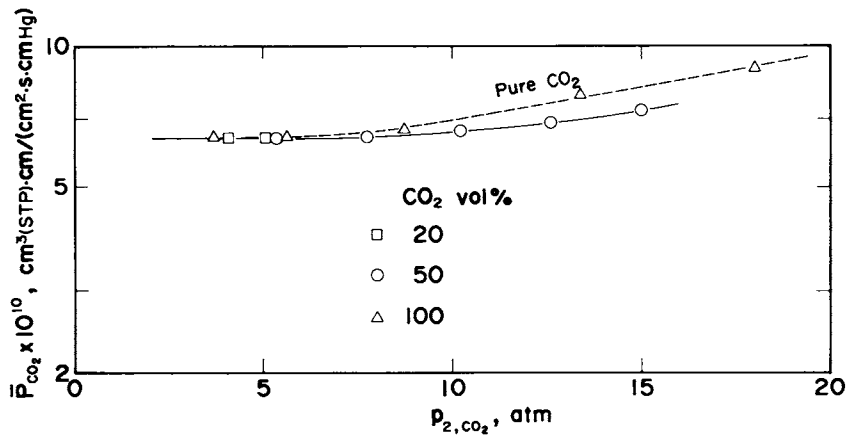

Figure 7 Dependence of permeability coefficient for CO_2 in a flat homogeneous membrane of cellulose triacetate on partial pressure of CO_2 in upstream at 30°C.

Since plasticization effect on cellulose triacetate membrane by CO_2 has been reported by several authors,[3,4,8,9] to make sure that the above result is valid, permeability measurements with homogeneous cellulose triacetate membrane for CO_2 and CO_2–air mixtures were conducted. The results are shown in Figure 7. It is obvious that pressure dependence of the permeability coefficient for CO_2 in the mixture becomes weaker than that for pure CO_2 at the same partial pressure of CO_2. This could be attributed to a competition among the penetrants for unrelaxed volume in the membrane.[8,10] Due to this effect, the solubility of CO_2 is reduced. The decrease in solubility can in turn reduce diffusivity. As a result, the permeability for CO_2 is lowered by the presence of air. Especially in the region below 8 atm (the pressure corresponding to the highest partial pressure of CO_2 in the separation experiments), the permeability coefficients practically do not change with increasing pressure. Therefore, it can be expected that in the separation experiments of this work, the change in permeability for CO_2 due to the plasticization effect can be neglected.

The deviations of the simulation curves from experimental data at low stage cuts appear to be larger than experimental errors and could be due to the fact that the assumption of negligible pressure loss in the bore side is not satisfied, as high permeate flux induces pressure buildup inside the bore.

Nevertheless, the good agreement between the calculated values and experimental data suggests that in the range of the present work, permeation data of the pure gases can be used to predict the separation performance of the cellulose triacetate hollow fiber membrane module, and separation factors close to calculated ones could be achieved.

CONCLUSION

The ideal separation factor of asymmetric hollow fiber membrane of cellulose triacetate for CO_2 relative to N_2 at 30°C ranged from 21 to 24. Permeation behavior for pure CO_2 was interpreted in terms of the total immobilization model, where the diffusion coefficient for Henry's law mode depends on gas pressure via a modified free-volume model, whereas that for pure O_2 and N_2 could be interpreted in terms of a simple solution diffusion model. Based on pure gas permeabilities to CO_2, O_2, and N_2, simulation for the separation of CO_2–air mixtures was conducted using a countercurrent plug flow model, and the result fitted the experimental data fairly well. Membrane plasticization induced by CO_2 has negligible effect on permeation to mixture of CO_2 and air in the range of CO_2 composition up to 50% and upstream total pressure up to 1.5 MPa.

NOMENCLATURE

A_t	total membrane area in the moule, cm^2
D_i	hollow fiber inside diameter, mm
D_0	hollow fiber outside diameter, mm
J_s	steady-state permeation flux, cm^3 (STP)/(cm^2 s)
L_t	total length of hollow fiber, cm
N_t	total number of hollow fibers in the module
$\bar{P}$	mean permeability coefficient, cm^3 (STP) cm/(cm^2 s atm) or cm^3 (STP) cm/(cm^2 s cmHg)
p	pressure, atm
p_1	permeate outlet pressure or downstream pressure, atm

p_2 feed-side pressure or upstream pressure, atm
y_P permeate concentration of CO_2 in mole fraction
α ideal separation factor of CO_2 relative to N_2
δ effective thickness of skin layer of asymmetric membrane, cm
Δp $= p_2 - p_1$, atm
θ stage cut defined as the ratio of permeate flow rate to feed flow rate
κ $= \bar{P}/\delta$, permeation rate coefficient, cm^3 (STP)/(cm^2 s atm) or cm^3 (STP)/(cm^2 s cmHg)

REFERENCES

1. E. Sada, H. Kumazawa, K. Nakata, N. Kawashima, S. Kataoka, and K. Tada, *J. Appl. Polym. Sci.*, to appear.
2. E. Sada, H. Kumazawa, and P. Xu, *J. Appl. Polym. Sci.*, **35,** 1497 (1988).
3. E. Sada, H. Kumazawa, Y. Yoshio, S.-T. Wang, and P. Xu, *J. Polym. Sci., Part B, Polym. Phys.*, **26,** 1035 (1988).
4. E. Sada, H. Kumazawa, P. Xu, and S.-T. Wang, *J. Polym. Sci., Part B, Polym. Phys.*, **28,** 113 (1990).
5. E. Sada, H. Kumazawa, P. Xu, and T. Nishikawa, *J. Appl. Polym. Sci.*, **33,** 3037 (1987).
6. S. T. Hwang and K. Kammermeyer, *Membranes in Separations,* Chapter 7, Wiley-Interscience, New York, 1975.
7. C. Y. Pan, *AIChE J.*, **29,** 545 (1983).
8. M. D. Donohue, B. S. Minhasm, and S. Y. Lee, *J. Membrane Sci.*, **42,** 197 (1989).
9. E. S. Sanders, *J. Membrane Sci.*, **37,** 63 (1988).
10. E. S. Sanders, W. J. Koros, H. B. Hopfenberg, and V. T. Stannett, *J. Membrane Sci.*, **13,** 161 (1983).

Received September 10, 1991
Accepted October 30, 1991